MONITORING OF A CERAMIC SURFACE TEMPERATURE FIELD INDUCED BY PULSED Nd:YAG LASER

Dragan M. KNEŽEVIĆ[1], Bojana M. RADOJKOVIĆ[2], Slavica S. RISTIĆ[3], Suzana R. POLIĆ[3],*
Milovan M. JANIĆIJEVIĆ[4], Ljubiša D. TOMIĆ[1] and Bore V. JEGDIĆ[2]

[1]Military technical institute, Belgrade, Serbia
[2]Institute of Chemistry, Technology and Metallurgy, University of Belgrade, Belgrade, Serbia
[3]Central Institute for Conservation in Belgrade, Belgrade, Serbia
[4]Metalac A.D. Gornji Milanovac, Serbia

Corresponding author: e-mail: s1avce@yahoo.com

Temperature distribution induced by laser radiation is a very important parameter for an efficient and safe application of lasers in different ceramic processing techniques. This paper presents the results of an infrared thermography (IRT) application for monitoring temperature distribution on a ceramic surface during Nd: YAG laser irradiation with different fluences and 8ns pulse duration. FLIR, E40 and SC7200 IR cameras were used with the aim of recording the maximum temperature in the irradiated zones. It was expected that IRT could give some information related to the heat affected zone and possible damage to the base material; however, the results have shown that IR cameras, even those with high performance such as SC7200, cannot record the maximum temperature value at the moment of laser operation, but only the average temperature of the bulk sample material after laser pulses. The results of the numerical simulation have confirmed the value of the thermographic measurements. The microstructure and micromorphology of the ceramic surface before and after the laser treatment were analysed by optical and scanning electron microscopy as well as by examining the roughness of the irradiated and non- irradiated surfaces, while the micromechanical changes were analysed by comparing the micro-hardness of the irradiated and non-exposed surfaces.

Keywords: *Laser, chemical properties, surface properties, scanning electron microscopy (SEM), numerical simulation*

1. Introduction

Thanks to the dynamic development of modern technologies in the 20th and the 21st century, lasers, as sources of coherent and monochromatic radiation of high intensity, have found numerous applications in science, industry, medicine, military and space programs, as well as in many everyday life areas. They are used in systems for digitizing objects, as tools in production plants, and in conservation studios [1-5]. Lasers can be used for surface cleaning, scribing, sintering, cutting, drilling, milling or marking; they can also be a light source in different diagnostic procedures. In ceramic processing, two types of lasers are used: CO_2 lasers that emit in the far-infrared region of the

spectrum, wavelength $\lambda = 10.6$ μm, and solid state lasers with output wavelengths ranging from the ultraviolet through the visible to the near-infrared (Nd: YAG) [3-9] .

Nd:YAG lasers are used in ceramic processing where CO_2 and other long wavelength lasers are unsuitable, especially in cases where high-quality processing and no thermal degradation are required, [8].

A ceramic is an inorganic, non-metallic and crystalline material. Many papers [5,6,9] confirm that ceramic materials have played an important role in human history. Ceramics are good thermal insulators with excellent chemical and thermal stability, high hardness, and good electric insulation, which is why they have many applications in electronics and structural engineering, medicine, aerospace, military equipment, and automotive industry.

Laser interaction with materials is a very complex phenomenon [1,3,5,7,9]. It has been a subject of many research works, but there are still many insufficiently known phenomena. Short pulse, nanosecond and sub-nanosecond Nd: YAG lasers open up a lot of possibilities for research in the field of laser-ceramic interaction.

A laser surface treatment of ceramics is an important application because it can enhance surface strength and roughness and improve the mechanical properties of the material. It could also be used for refinement of microstructures, dissolution of inclusions, laser cladding, and the formation of quasi-crystalline and amorphous materials [9] as well as microstructural changes, that often leading to improved corrosion resistance.

Real-time monitoring of laser processing is important for optimizing processes and avoiding potential sources of damage. The monitoring process can be performed automatically by CCD cameras, infrared (IR) cameras, spectroscopy (LIBS, LIF), or other techniques [10-14].

All objects emit IR radiation at temperatures above absolute zero. The amount of radiation increases with temperature. IR cameras can convert IR radiation (0.9–14 μm) to visual images that show thermal variations across an object as different colours or shades of grey. IR thermography is one of the most used techniques for non-destructive testing in many areas of science and industry. Alone, or combined with other methods, IR thermography can detect surface temperature, heat loss, moisture in walls and roofs, thermal insulation, structural damage, medical problems…[11-19].

This paper presents some results of a ceramic tile surface treatment by Nd: YAG laser with different fluences (Tab. 1). The laser-induced heat propagation was determined using FLIR E40 and SC7200 thermographic cameras. To evaluate the results of the laser impact, several analytical techniques were used.

Numerical methods are a very useful tool in engineering [20-22]. In this research, numerical simulations were used together with thermography to determine the temperature field induced by laser irradiation on the surface of a ceramic tile.

2. Laser- ceramics interaction

The laser beam can interact with a ceramic surface producing various effects, depending on the laser parameters such as wavelength, polarization, intensity, pulse duration, pulse repetition, and beam homogeneity, as well as on the properties of the surface such as coefficient of absorption, thermal relaxation time, thermal diffusivity, thermal conductivity, specific heat and latent heats of melting and evaporation, morphology, topography, temperature, and wetting [23-31]. Ceramic processing with

lasers is characterized by high energy density and directionality, which permits a strongly localized heat treatment of a material with a spatial resolution better than 100nm. For longer pulses, absorbed energy will be dissipated into the surrounding material by thermal processes. Absorption of long laser pulses also causes melting and substantial sputter evaporation of the material. These phenomena can contaminate the surrounding area, produce micro cracks, and remove the material the size of which is much larger than the laser spot dimensions.

There are several parameters important for laser processing: selection of a wavelength with a minimum absorption depth, pulse duration to maximize peak power and to minimize thermal conduction to the surrounding work material, pulse repetition rate, laser beam quality, and homogeneity of energy, focus ability, and controllability of the spot size. The atmospheric conditions are very important for both the mechanism and the results of a laser treatment.

The advantages of the laser processing of ceramics are: possibility of high accuracy, spatial and temporal control, and immediate change of laser parameters, material selectivity, and ecologically friendly characteristics [27-31]. However, very often, the thermal nature of the interaction causes unwanted side effects such as: chemical decomposition, thermal stresses, micro-cracking, melting and rapid re-solidification of the amorphous material. A special attention has been therefore paid to control the operation parameters that enable a safe application of laser procedures on ceramics. Many studies confirm that Nd: YAG lasers with wavelength λ = 1.06 nm and ns pulses duration are highly effective in surface processing; however, the absorption of laser radiation by bulk material can raise the surface temperature and cause some changes in morphology and chemical composition.
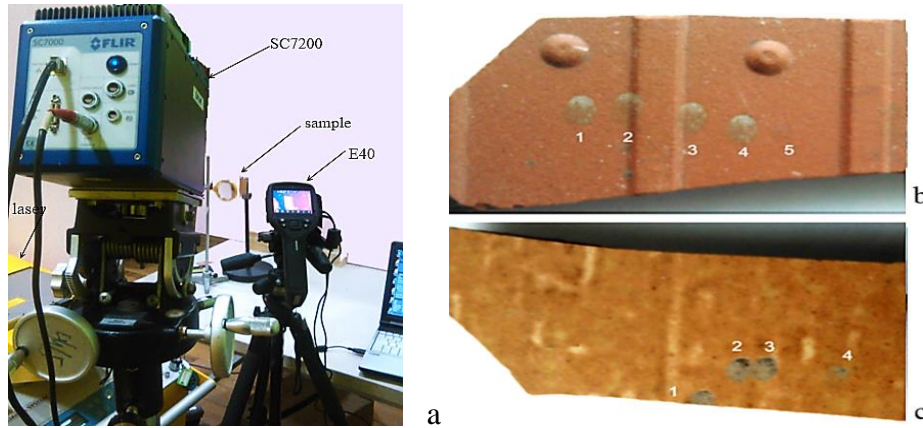
3. Experiment

The experiments were performed using Nd: YAG laser, Thunder Art Laser, a product of Quanta System. The laser operates in the Q-switch mode with three λ: 1064 nm, 532 nm, and 355 nm. The duration of a pulse was τ = 8 ns. The repetition rate was f_l = 1-20 Hz. An unfocused laser beam had 10 mm in diameter and the Gaussian distribution of energy. The maximum energy of the laser beam, for λ = 1064 nm, was E = 750 mJ. The laser system has a mobile, articulated arm through which the laser beam is conducted with the aid of seven mirrors. The laser beam was focused by a lens with 150 mm focal length. The tested sample was positioned in front of the lens focus (Fig.1a).

Two FLIR IR cameras, E40 and SC7200, were used in parallel for monitoring and recording the surface temperature during the laser treatments. The cameras were in the off-axial thermography setup.

The characteristics of used IR cameras can be found in manufacturers' documentations [11].

A piece of a ceramic tile with the zones of interaction, after the laser irradiation, is presented in Fig. 1b and Fig.1c. The front side of the sample has a glazed layer, while the back side is unglazed.

Table 1 presents the most important laser parameters during the experiments and the settings of the IR cameras for temperature monitoring during the laser treatments. The experiments were performed under normal atmospheric conditions. In Tab. 1, F is fluence, I_t is integration time, t duration of treatment, N number of recording, f is frame rate, ΔT temperature range of camera and T_{max} is maximum of temperature in irradiated zone.

Figure 1 a-Experimental setup, a piece of ceramic tile with laser irradiated zones on b-unglazed and c-glazed side

The ceramic surface structure and morphology were studied on an USB optical microscope (OM) and a scanning electron microscope (SEM). The SEM was connected to an INCA350 energy-dispersion spectroscope (EDX). The EDX analysis was used for the determination of the changes in the material composition of the irradiated zones. The sample composition was analysed by an X-ray fluorescence (XRF) spectrometer (model: XL 3t 900He, Thermo Fisher Scientific) with a standard analytical range. The micro-morphological changes were analysed by examining roughness with TIME Instruments TR200 profilometer, while the micromechanical changes were determined by comparing the microhardness before and after the laser treatment using (Micro Vickers Hardness Tester: TH710).

A numerical simulation of temperature changes on the glazed surface was performed for the experimental conditions during the laser treatment of zone 3 (Tab. 2). The COMSOL Multiphysics software package was used with the aim of defining the temperature distribution within the irradiated zone and around it. The experimental conditions were the input data in the numerical simulations. The results were compared and used to verify the applied methods.

4. Results and discussion

This paper presents the results of a ceramic tile surface treatment by Nd:YAG laser with $\lambda = 1.06$ and different fluences. The analysis of the laser impact effects shows that, in most cases, irreversible microscopic and macroscopic changes have occurred on the glaze or in the ceramic body material. The applied fluences in the experiments were close to the damage threshold for the ceramic tile. The ceramic tile emissivity of $\varepsilon = 0.9$ was determined in accordance with the FLIR Manual [11], with a known, high emissivity electrical tape.

The parameters of laser and IR cameras settled during experiments and measured Tmax are givend in Tab. 1.

Figures 2 and Figs 3 show the results of the thermographic recordings by E40 and SC7200 cameras, respectively. The ResearchIR software [11], is used for presenting the temperature visualization and the measurements. Figure 2 presents the temporal plot for a point with the maximum temperature value; Fig. 2a for zone 1, and Fig.2b for zone 5, on unglazed side (Fig.1b). Since the integration time of an E40 camera is 20ms, the average value and the measured temperature is lower in

comparison to the average temperature measured with an SC7200 camera which has the integration time of: 20, 60 or 120 μs (Figs 3a-3d and Tab. 1).

**Table 1 Experimental data for the laser surface treatment temperature monitoring**

	Laser parameters					E40			SC7200				
zone	λ, [nm]	E, [mJ]	F, [J/cm^2]	f_l, [Hz]	t, [s]	N	ΔT [°C]	T_{max} [°C]	N	f, [KHz]	I_t, [μs]	ΔT[°C]	T_{max}, [°C]
Unglazed surface													
1	1064	750	4.0	20	2.6	230	-20-120	117.7	1568	1	20	117-239	250
2		600	3.2		2.8	231		102.1	1569		60	66-161	180
3		450	2.4		2.9	232		85.0	1570		150	27-110	126
4		500	2.6		4.0	233		95.1	1571		120	37-122	140
5		300	3.1		2.3	236		68.5	1578		120	37-122	90
Glazed surface													
1	1064	750	4.0	20	3.7	246	-20-120	114.1	1586	1	20	117-239	270
2		750	4.0		4.3	247		>150	1587		20	117-239	280
3		600	3.2		4.1	248		147	1588		60	66-161	200
4		450	2.4		3.7	249		81.9	1589		40	66-161	140

Table 2 Main thermal-physical parameters for the numerical simulation

ceramics	Density, ρ, [kg/m^3]	Specific heat [J/kgK]	Thermal conductivity [W/mK]	Thermal expansion coefficient $\cdot 10^{-6}$	Reflection coefficient
Glazed	2350	750	1.5	5.4	0.81
Unglazed	2350	750	1.5	5.1	0.84

The lack of synchronization between the laser pulses and the beginning of the camera's recording caused a temperature difference generated from the pulse with the same energy (Fig. 3). Apart from synchronization, the accuracy of the temperature measurements depends on the choice of integration time, and the temperature range of the camera. Diagrams 3a and 3b refer to zone 1(Fig.1b), taken with different temperature ranges, so the obtained mean temperature values also differ.
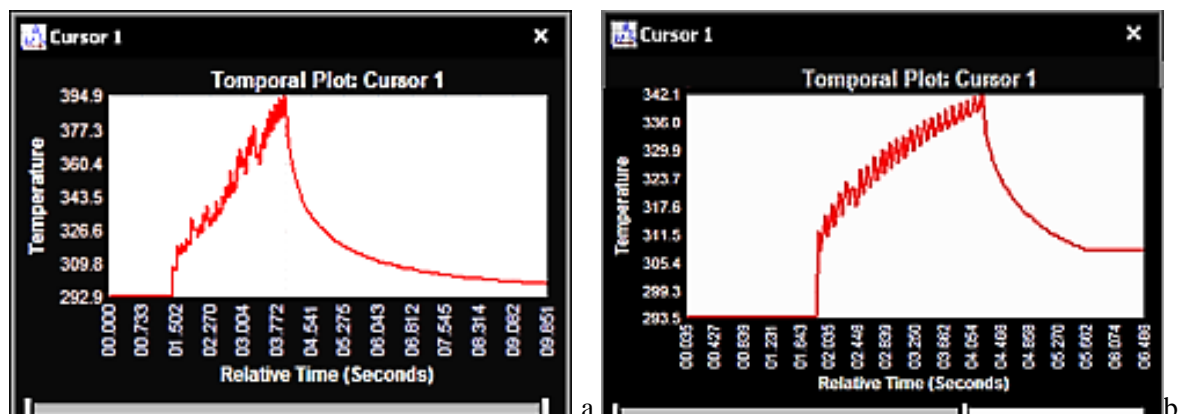

Figure 2 Temperature diagrams (IR camera E40) recorded for; a-zone 1, b- zone 5 (fig. 1b)

IR cameras setting parameters as I_t and ΔT have important influence on measured T_{max}. It is possible to adjust the camera's integration time or temperature range to the desired value, but if the integration time is chosen, the temperature range will be automatically adjusted.
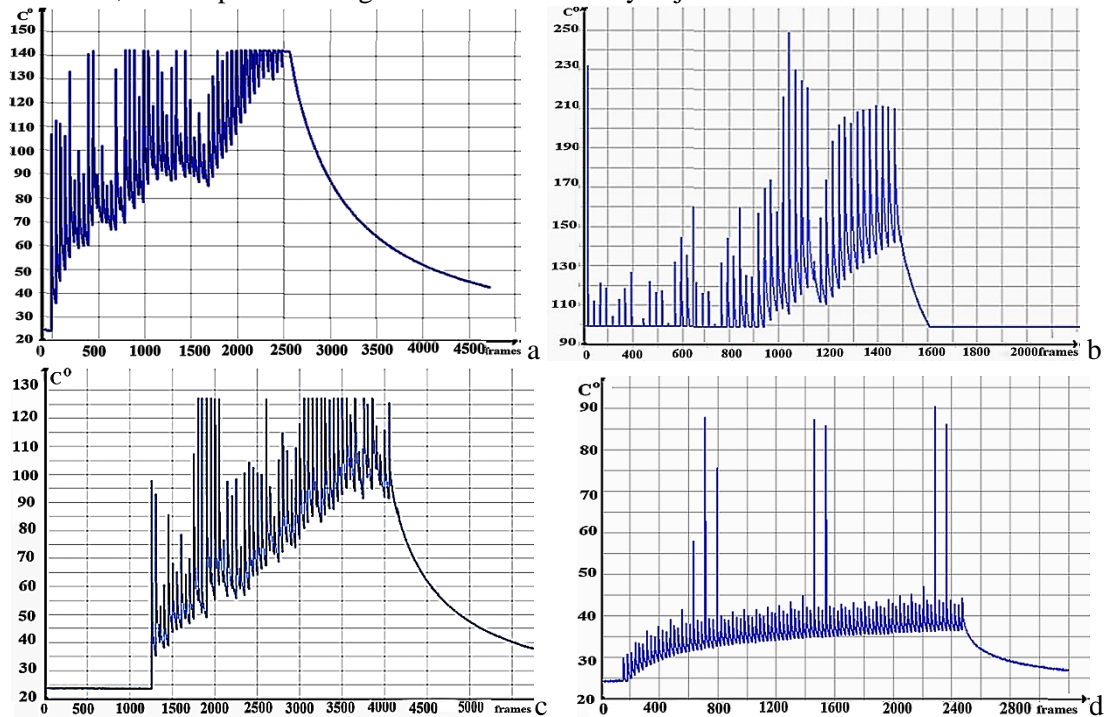
Figure 3 Temperature changes recorded by SC7200 camera; a and b- zone 1, c- zone 2 and d- zone 5 (Fig.1b)

With aim to investigate the influence of the camera sampling rate on the maximum temperature measurement, the set of experiment were performed and some results are presented in Fig. 4. It was showed that the frequency of camera sampling does not have significant influence on maximum temperature measurement, only on the recorded bursts with T_{max}.
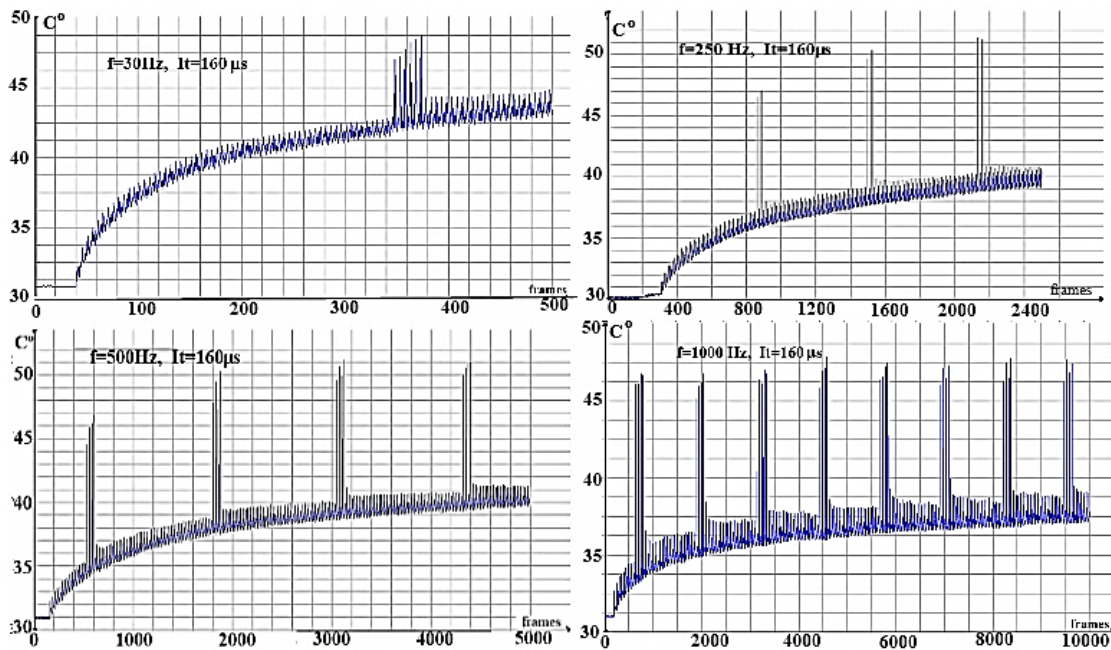
Figure 4 The results of temperature measurement on the zones iradiated with $\lambda = 1064$ nm, E = 250 mJ and $f_l = 20$ Hz and different camera sampling frequencies.

6

The optical microscopy and the SEM images of the unglazed side (zones 1, 3 and 5) are presented in Fig. 5 - the whole zone, the upper part of the zone and the right one. Laser energy induced colour changes on the unglazed side.
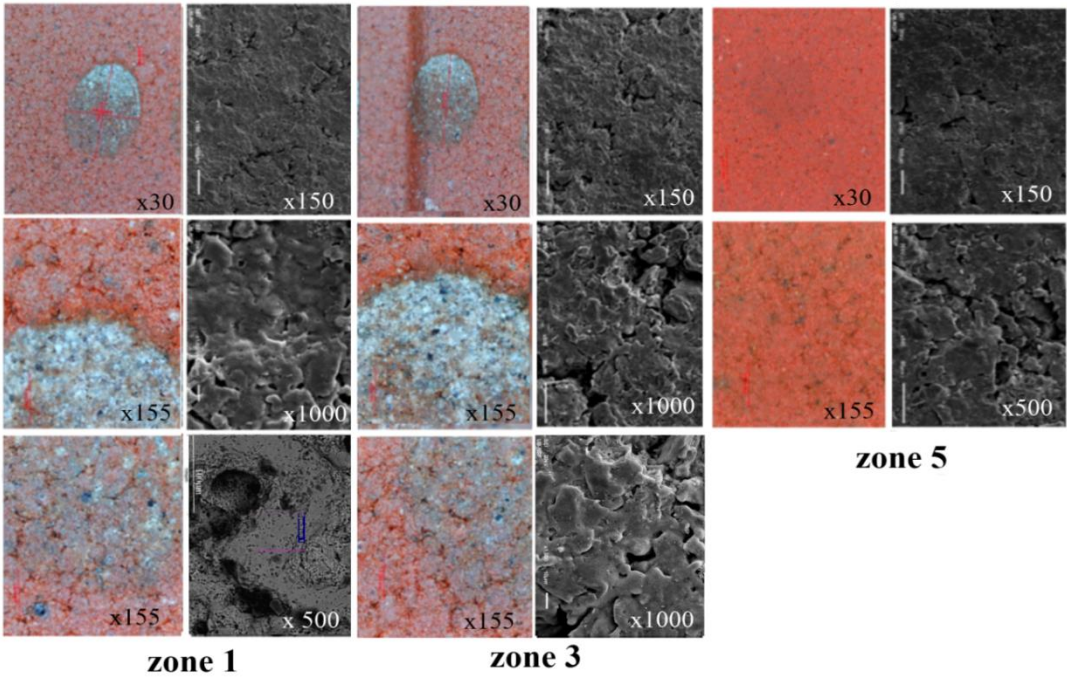

Figure 5 OM and SEM images of zones 1, 3 and 5 on unglazed ceramics side (Fig. 1b)

Zone 1, irradiated with 4 Jcm^{-2}, shows some surface damage. The damage threshold is lower than expected. According to the optical microscopy results, the surface seemed undamaged at this fluence, but SEM images confirm the damages in left side. The right part of the irradiated area remained undamaged. It may be related to the non-uniform laser beams profile and it could be avoided if an appropriate mode structure (a beam distribution profile) is used.

Figure 6 shows the surface temperature changes of zones 2 and 4 on the glazed side, during laser irradiation, recorded by E40 camera, while Fig. 7 shows the diagrams of temperature variations versus time of impact for zones 1 and 3 (Fig.1b), recorded by SC7200 camera. The experimental results (Fig. 7b) show that an SC7200 IC camera, with the integration time of 60μs, measured 190 and 200 °C (483 K and 493K) for some laser pulses. In an ideal case of laser and camera synchronization, all recorded pulses would probably reach the same average temperature.
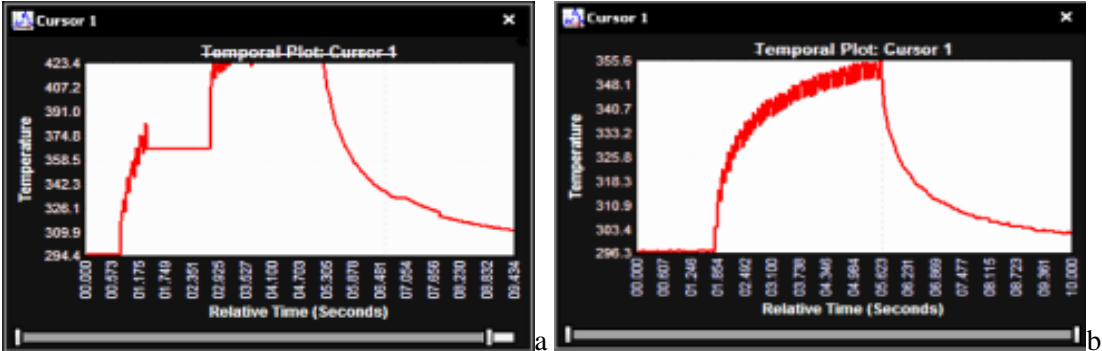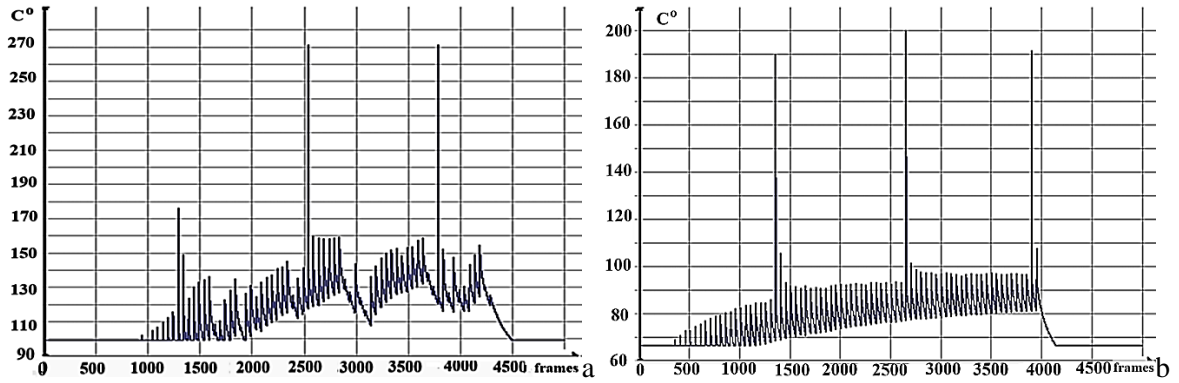

Figure 6 Temperature diagrams (Temporal plots, IR camera E40 and Researcher IR softwere) recorded during treatment of a- zone 2 and b- zone 4 on glazed side (Fig.1c)

7

Figure 7 Temperature changes recorded by SC7200 camera in: a-zone 1 and b-zone 3(Fig.1c)

The SEM images of two zones, 2 and 4, are given in Fig. 8. It is evident that the ceramic glaze was dissolved and again hardened (zone 2).The same happened in zone 4, only on a smaller surface.
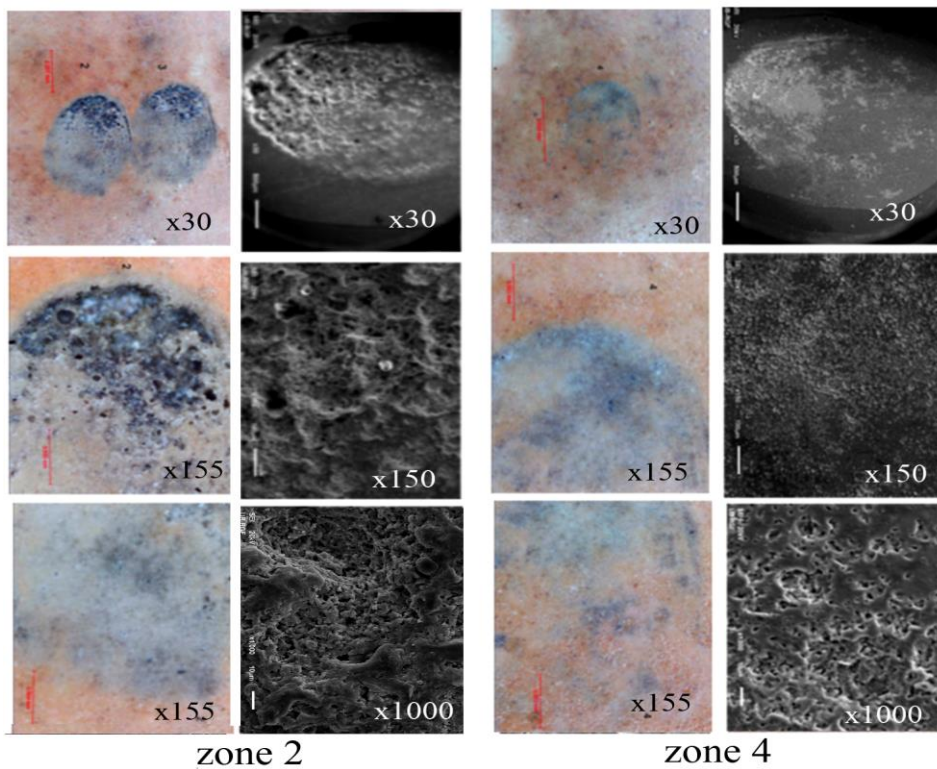
Figure 8 OM and SEM images of laser irradiated zones 2 and 4, on glazed surface (Fig.1c)

The numerical simulation results of temperature changes, on the glazed surface, performed for the experimental conditions during the laser treatment of zone 3 (Tab. 2) are presented in Fig. 9, where Fig. 9a shows 2D distribution of the surface temperature during 50µs from the beginning of laser pulse with 3.2 J/cm^2 fluence, $\tau = 8$ ns, and $\lambda = 1064$ nm, while Fig. 9b shows the surface temperature during the first 1 µs.

In the zone 3, the maximum temperature is 524 K at time 0.3 µs, and after 50 µs it decreases to 458 K. The temperature gradient, in zone 3, is 1.32 K/µs. It means that, after 60 µs, the expecting temperature may be 445 K. The average temperature value for a period of 60µs is approximately 485 K. The IR camera 7200 has measured average temperature 200 °C (473 K).

8

The difference between the numerical values for the mean temperature and the values obtained by the SC7200 camera is about 10%, and the values measured by the E40 camera are about 40% lower.

The numerical 2D temperature distribution on the ceramic surface for zone 3 (Fig.1b) is shown for 0.29µs (Fig. 9c) and for 38µs (Fig. 9d) after the laser pulse beginning.
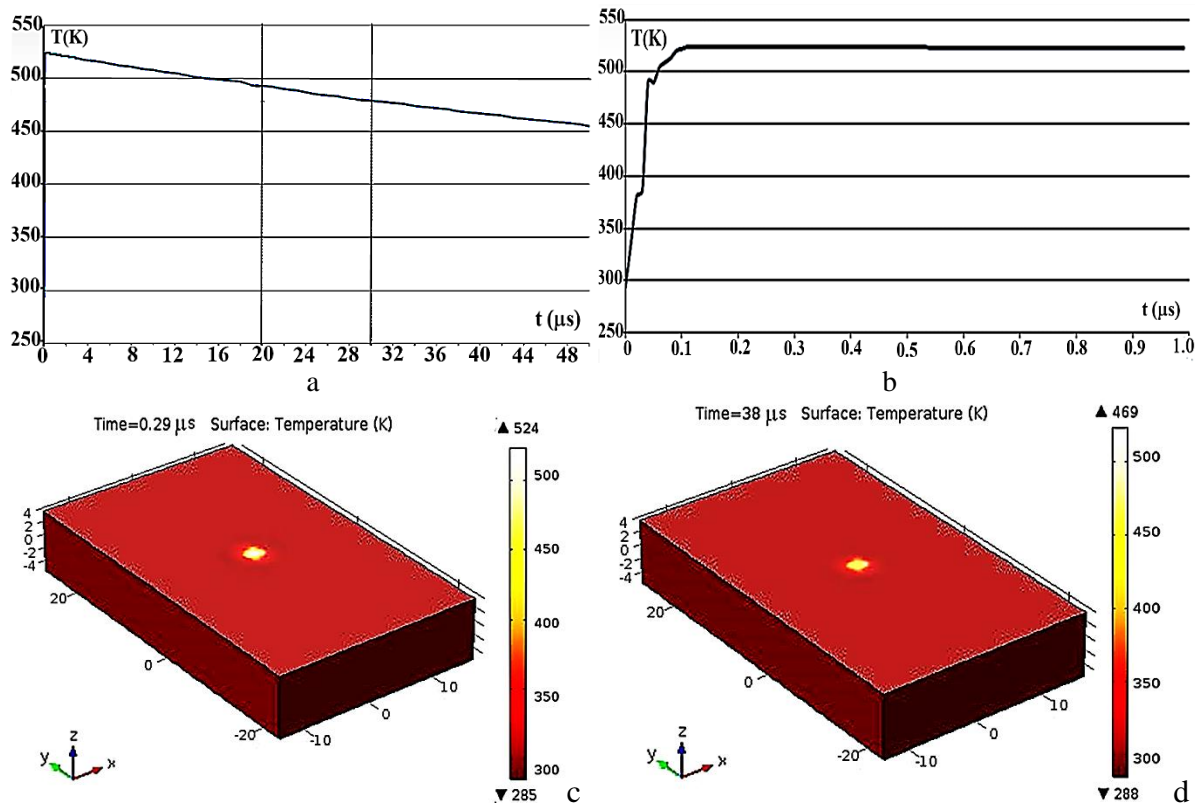
Figure 9 Numerical temperature distributions on glazed surface in zone 3 (Fig. 1b)

The XRF and EDX methods were used to study the composition of the ceramic tile, the glaze and the bulk material. The XRF results, in Tab. 3, present S as SO_3. Actually, SO_3 does not exist as a component in ceramics, but as a hexavalent S ion, which, in reaction with other ions, gives sulphates

Table 3 Results of the XRF analysis.

compound [wt%]	Na_2O	MgO	Al_2O_3	SiO_2	P_2O_5	SO_3	K_2O	CaO
Unglazed	1,17	1,34	21,95	62,53	0,273	0,313	3,15	0,625
Glazed side	0,847	0,588	6,39	39,36	0,0794	0,0	1,21	0,820
Compound [wt%]	TiO_2	Fe_2O_3	NiO	CuO	ZnO	ZrO_2	PbO	SnO_2
Unglazed	1,08	7,13	0,0068	0,0051	0,0385	0,0776	0,0544	0,0
Glazed side	3,43	1,54	0,0	0,0118	2,22	23,21	18,60	1,00

The EDX analysis (Tab. 4) has confirmed that there are no significant changes between the lasers irradiated surface and unirradiated surface.

Laser surface hardening, one of the most widely used methods can be applied to metallic materials [30], locally or on the whole material. Nd:YAG and diode lasers are widely used lasers for hardening in different industries. A possibility to control laser parameters easily, process automation, low energy in comparison with classical methods, and good reproducibility are some advantages of laser hardening. The laser impact on the ceramic surface leads to different hardness values. Some

average results of the hardness measurements in the zones, both laser treated and not, are presented in Tab. 5. The results of the study show that hardness has increased in the zones treated with laser relative to the non-treated zones.

Table 4 EDX results for the glazed side (all results in weight %)

Spectrum	N	O	Na	Al	Si	Cl	K	Ca	Ti	Fe	Zn	Zr	Pb	Total
						zone 2								
Spectrum 1		34.46	1.20	3.64	22.38		0.86	1.14	1.87	1.39	2.82		30.23	100.00
Spectrum 2		38.12		2.33	16.75		0.55	0.73	1.83	1.15	2.27	15.82	20.44	100.00
						Unirradiated surface								
Spectrum 1		39.19		3.33	19.91		0.99	0.78	2.78	1.15	2.39		29.47	100.00

Table 5 Results of the hardness measurements

Side	Hardness by Vickers, HV	
glazed side, load 1.96 N	non-irradiated surface	551.3
	zone 2	598.7
Unglazed side, load 9.8 N	non-irradiated surface	479.85
	zone 1	560.65

Profilometric measurements were performed with TIME Instruments TR200 profilometer, in order to examine the changes of surface roughness in the areas treated by laser. Measurements were also carried out in several places that were not irradiated. Fig. 10a shows the measurements made on the untreated surface of the glazed side, and Fig. 10b shows roughness in zone 2 (glazed side). The appearance of the roughness profiles for the unglazed side in zones 1 and 5 is given in Figs 10c and 10d. On the glaze, there was an increase in roughness in all laser-treated zones, while roughness decreased on the unglazed side proportionally with increasing the applied laser fluence.
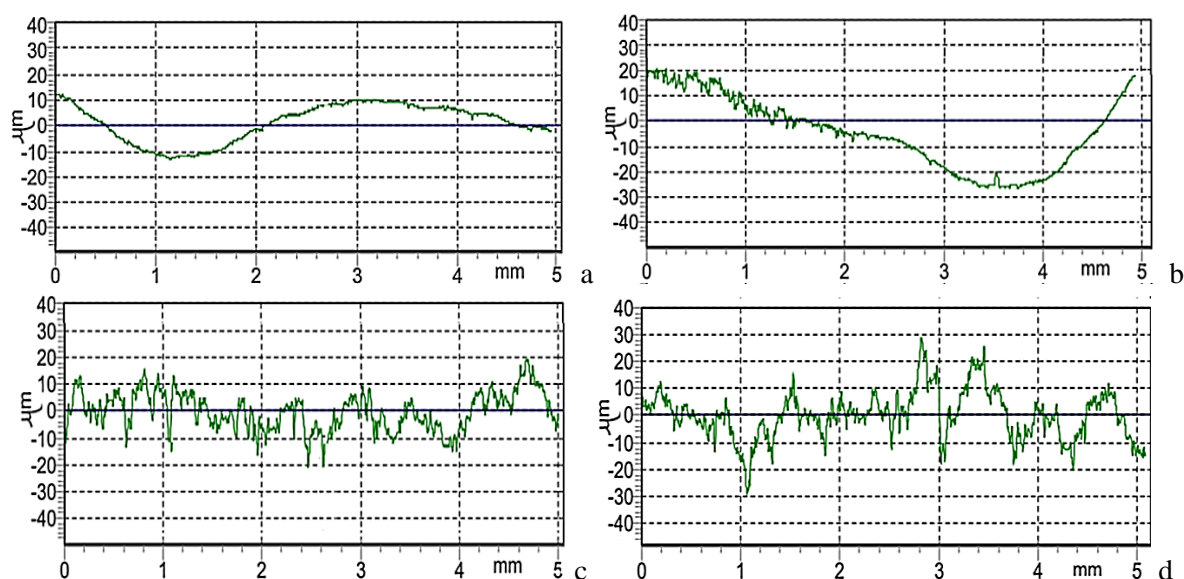
Figure 10 Roughness profiles on the glazed side (a and b) and the unglazed side (c and d) of the ceramic sample

5. Conclusion

This paper presents the results of an attempt to use infrared thermography for monitoring temperature distribution on a ceramic surface during NdYAG laser treatments with different fluences. It was expected that infrared thermography could give some information related to the heat affected zone and possible damage to the base material. E40 and SC7200 IC cameras were used with the aim of recording the maximum temperature in the irradiated zones, but the results have shown that IC cameras, even those with high performance such as SC7200 cameras, cannot record the maximum temperature value at the moment of laser operation, but only the average temperature of the bulk sample material after laser pulses. The results of the numerical simulation have confirmed the value of the thermographic measurements. The measured temperature depends on the camera integration time and temperature range. The frequency of camera sampling does not have significant influence. The synchronization of laser and camera sampling could optimize temperature measurement.

The analyses of the microstructure and micromorphology changes of the ceramic surface after the laser treatment were carried out by optical and scanning electron microscopy as well as by examining the roughness of the irradiated and non-irradiated surfaces, while the micromechanical changes were analysed by comparing the microhardness of both the irradiated and non-exposed surfaces. Both methods have shown that there are micromorphological changes that result from thermal energy induced by laser radiation, and that it is necessary to use methods that will precisely monitor the induction of heat in real time.

References

1. Bass, M., *Laser Material Processing*, North Holland, Amsterdam, 1983
2. Singh, S.C., et al., Chapter, Lasers: Fundamentals, Types, and Operations in Nanomaterials: Processing and Characterization with Lasers, S. C. Singh, et al., W. Cai (Eds.), Wiley-VCH Verlag and Co. KGaA, 2012
3. Webb, C., Jones, J., Handbook of Laser Technology and Applications, Taylor & Francis, 2003
4. Advanced Lasers, Editors:Shulika O., Sukhoivanov I., Springer, ISBN 978-94-017-9481-7 (eBook), 2015
5. Ristic, S. et al.. Analysis of ceramics surface modification induced by pulsed laser treatment, *Processing and Application of Ceramics,* 8 (2014), 1, pp. 15–23
6. Polić, S., et al, Studies of the Iranian medieval ceramics surface modified by pulsed TEA CO2 and Nd:YAG lasers, *Ceramics International*, 41 (2015), pp.85–100
7. Rey-García F., et al. Microstructural characterization and tribological behavior of Laser Furnace processed ceramic tiles, *Ceramics International*, 44 (2018), 6, pp. 6997-7005
8. Li, L., The Challenges Ahead for Laser Macro, Micro and Nano Manufacturing, *Advances-in-Laser-Materi. Processing*, chapter 2, 2018, pp. 23-42

9. Montealegre, M.A., et al., Surface treatments by laser technology, *Contem. Materials,* I−1 (2010), pp.20-30

10. Milošević, N., Application of the Laser Pulse Method of Measuring Thermal Diffusivity to Thin Alumina And Silicon Samples In A Wide Temperature Range, *Thermal Science*: 14, (2010), 2, pp. 417-423

11. ***Flir Systems, FLIR T-Series, www.flir.com (visited 15.10.2016)

12. Bagavathiappan, S., et al., Infrared thermography for condition monitoring – A review, *Infrared Phys. Techn*, 60 (2013), pp. 35–55

13. Polić, S., et al., Optimizacija laserskog čišćenja metalnih artifakta, *Tehnika*, 68 (2017), 6, pp.834-844

14. Radojković B., *Physico-mechanical and micro-chemical changes on the ceramic and metal artefacts surfaces treated with laser*, University of Belgrade, Faculty of technology and metallurgy, doctoral dissertation, 2017. (in Serbian)

15. Linić, S. Lj., et al.: Boundary-Layer Transition Detection by Thermography and Numerical Method Around Bionic Train Model In Wind Tunnel Test, .*Thermal Science*: 22, (2018), 2, pp. 1137-1148

16. Tomić, Lj. D., et al.: Application of Pulsed Flash Thermograpy Method for Specific Defect Estimation In Aluminum , *Thermal Science*, 19 (2015), 5, pp. 1845-1854

17. D. Knežević, et al., Minimum resolvable temperature difference model, simulation, measurement and analysis, Opt Quant Electron 48 (2016), 332. https://doi.org/10.1007/s11082-016-0598-7

18. Madić, M. J., et al.: Analysis of the Heat Affected Zone in CO2 Laser Cutting of Stainless Steel, S364 *Thermal Science*, 16, (2012), 2, pp. S363-S373

19. Khodayar, F., et al., Parameter Optimization of Robotize Line Scan Thermography for CFRP Composite Inspection, *J Nondestruct Eval* , (2018) 37: 5. https://doi.org/10.1007/s10921-017-0459-8

20. https://www.comsol.com/release/5.4 (10.07.2019.)

21. Janićijević, M., et al., Evaluation of laser beam interaction with carbon based material - glassy carbon, *Chem. Ind. Chem. Eng. Q.* 21 (2015), 1, pp.63−69

22. Kranjc, M., et al., Numerical analysis and thermographic investigation of induction heating, *International Journal of Heat and Mass Transfer*, 53 (2010), 17–18,pp. 3585-3591

23. Sartinska, L.L., et al., Laser induced modification of surface structures, *Appl. Surface Sci.*, 253 (2007), pp. 4295–4299.

24. Costil, S., et al., Surface modification of ceramic matrix composites induced by laser treatment, *Appl. Surf. Sci.*, 255 (2008), pp. 2425–2432

25. Gurauskis, J., et al, Laser-assisted, crack-free surface melting of large eutectic ceramic bodies*, J. Eur. Ceram. Soc*. 31 (2011), pp. 1251–1256

26. Meijer, J., Laser beam machining (LBM), state of the art and new opportunities, *J. Mater. Process. Tech.*, 149 (2004), pp. 2–17

27. Ristic, S., et all, Some Experimental Results of Ruby Laser Beam Interaction with Neolithic Ceramics from Stubline, Serbia, *Laser engineering,* 23 (2012), pp.403-412

28. Nedialkov, N., et al., Analysis of surface and material modifications caused by laser drilling of AlN ceramics, *Appl. Surf. Sci.*, 254 (2007), pp. 893–897

29. Shukla, P., Lawrence, J., Characterization and modification of technical ceramics through laser surface engineering, *Laser Surface Engineering Processes and Application*s, Woodhead Publishing Series in Electronic and Optical Materials, 2015

30. Radojković, B., et al., Studies of pulsed tea CO_2 and Nd:YAG lasers applicaton in the ceramics surface conservation, *Ecologica*, 21 (2014), 75, pp.555-552

31. D. Sola, J. I. Peña, Study of the Wavelength Dependence in Laser Ablation of Advanced Ceramics and Glass-Ceramic Materials in the Nanosecond Range, *Materials* (Basel), 6 (2013), 11 pp. 5302–5313